Watenphul, A., Wunder, B. (2010): Temperature dependence of the OH-stretching frequencies in topaz-OH. - Physics and Chemistry of Minerals, 37, 65-72

DOI: 10.1007/s00269-009-0310-6

Temperature dependence of the OH-stretching frequencies in topaz-OH

Anke Watenphul and Bernd Wunder

Deutsches GeoForschungsZentrum (GFZ), Telegrafenberg, 14473 Potsdam, Germany,
Section 3.3 email: watenphul@gfz-potsdam.de

Abstract

Hydrogen bonding in topaz-OH, $Al_2SiO_4(OH)_2$, was investigated by IR spectroscopic analysis of the temperature dependence of the OH-stretching frequencies. Low-temperature spectra ranging from –196 to –160°C prove the existence of four non-equivalent H-positions in the crystal structure from the occurrence of four different OH-bands. With increasing temperature, these bands merge first, above –160°C, into two OH-bands and then above 400°C into one asymmetric broad band. Shifting of the OH-bands is caused by thermally induced hydrogen order–disorder. Low temperature fixes the protons in their positions; increasing temperature induces proton movement and allows switching between the different positions. Autocorrelation analysis of the IR spectra reveals two phase transitions, one at about –155°C from *P1* to $Pbn2_1$ characterized as static–dynamic change and the second at about 380°C from $Pbn2_1$ to *Pbnm* caused by disordering of the protons. The increasing symmetry with temperature is due to advanced proton movement and dynamical averages over the proton distribution densities.

Keywords Topaz-OH · IR spectroscopy · Autocorrelation analysis · Order–disorder phase transition

Introduction

Topaz, $Al_2SiO_4(F,OH)_2$, is a well-known hydrous mineral in aluminous and fluorine-rich rocks occurring in near-surface environments (e.g., Ribbe 1982); less often it is also found in low-temperature, high- to ultrahigh-pressure metamorphic rocks (Theye 1988; Zhang et al. 2002). The range of the (OH,F)-solid solution was previously thought to be limited up to $X_{OH} = 0.5$ [$X_{OH} = OH/(OH + F)$] due to proton–proton avoidance (Barton 1982). However, finding of OH-rich topaz with $X_{OH} = 0.55$ in samples from ultrahigh-pressure rocks of the Sulu terrane, eastern China (Zhang et al. 2002), as well as experimental studies at high pressure indicate that depending on the P–T–X-conditions, topaz might be stable along the complete (OH,F)-solid solution series (Wunder et al. 1993, 1999). The existence of topaz with $X_{OH} = 1.0$ was first predicted from energy calculations (Abbott 1990) and confirmed later by high-pressure synthesis (Wunder et al. 1993). Since then, the fully hydrated end-member of topaz, $Al_2SiO_4(OH)_2$, is termed topaz-OH. The stability of topaz-OH in the $Al_2O_3 - SiO_2 - H_2O$–system has been reported at pressures between 5.5 and 13 GPa and temperatures up to 1,500°C (Wunder et al. 1993; Ono 1999). Topaz-OH is suggested to be an important water carrier in pelitic sediments and basaltic rocks, which are subducted to depths below 150 km (Schreyer 1995; Schmidt 1995; Domanik and Holloway 1996; Ono 1998).

The hydrogen-bonding geometry of topaz-OH is controversial discussed. X-ray studies of topaz-OH and its deuterated analog, topaz-OD, using single crystal X-ray (Northrup et al. 1994) and neutron powder diffraction (Chen et al. 2005; Komatsu et al. 2008) indicated that hydrogen is located in two non-equivalent sites. In contrast to that, Churakov and Wunder (2004) predicted the existence of four non-equivalent proton positions, H1–H4, from ab initio quantum mechanical calculations. At ambient conditions, the four protons are in dynamic exchange between the allowed positions of local minima. Flipping of the protons between different sites is achieved by simple rotation of the OH-dipole between the closely adjacent H4 and H1 as well as H3 and H2 positions, which corresponds to the two observed OH-bands in the IR spectrum, respectively. This prediction is supported by NMR- and Raman investigations on topaz-OH (Xue et al. 2006).

The aim of the present work is to clarify the OH-bonding geometry in topaz-OH and its temperature dependence using IR spectroscopy and the autocorrelation method.

Experimental and analytical techniques

Experimental setup

For synthesis of topaz-OH, we used a stoichiometric $Al_2O_3 - SiO_2$–gel plus 20 wt% of bidistilled water as starting materials. The gel was dried for 1 h at 700°C before usage. The gel and fluid were loaded into a gold capsule, which was then cold-welded. Topaz-OH was synthesized in a rotating multi-anvil apparatus at 900°C, 10 GPa, and a run duration of 50 h. To prevent separation of fluid and solid components, experiments were performed at 360°-rotation of the Walker-type module with a speed of 5°/s. The experiment was performed with a 14/8 assembly (octahedron edge length/anvil truncation edge length). The temperature was measured using a W5%Re–W26%Re (Type C) thermocouple with a pre-

cision of about ±10°C. The pressure calibration was performed by press–load experiments based on room and high-temperature phase transitions. The estimated pressure uncertainty is about ±0.2 GPa. A detailed description of the synthesis method and the assembly set up is given in Watenphul et al. (2009). After the experiment, the capsule was separated from the assembly material, cleaned in an ultrasonic bath for 10 min in ethanol and then carefully opened.

Analytical methods

Powder X-ray diffraction

The run product was characterized by powder X-ray diffraction (XRD) in the 2θ–range 5–125° using a STOE STADI P diffractometer with a CuKα_1-radiation source. The collected pattern was processed using the GSAS software package for Rietveld refinement (Larson and von Dreele 2004) for phase identification and refinement of unit cell parameters.

IR spectroscopy

The topaz-OH crystals were up to about 10 μm × 25 μm in size, which is too small for a single-crystal IR analysis. Therefore, about 0.5 mg of the crystals was powdered in an agate mortar. Subsequently, a small pinch of the powder was spread on one diamond of a diamond anvil cell (DAC). The DAC was closed and the powder was pressed to a thin film with a pressure of about 2–3 GPa. This preparation method has several advantages: (1) the sample film has a constant thickness, which can be used to calculate the OH concentration with the Lambert–Beer-law and (2) any possible preferred orientation of the crystals is minimized. The film was then mounted on a glass carrier. The film thickness was determined to 3 ± 0.5 μm by analysis of video images using the program OPUS by Bruker. The film on the glass carrier was then mounted into a Linkam FTIR600 heating/freezing stage.

Unpolarized IR spectra were collected in the spectral range 4,000–3,000 cm^{-1} between –196 and 600°C using a Bruker IFS 66v FTIR spectrometer and a Hyperion IR microscope. The resolution was 1 cm^{-1} using a Globar light source, a KBr beamsplitter and a MCT-detector. The spectra were taken with an aperture of 40 μm × 40 μm and averaged over 256 scans. The interferograms were phase-corrected after the procedure of Mertz (1965) and Griffiths and de Haseth (1986). Blackman–Harris 3-term mode was chosen as apodization function. The measured spectra were transformed into absorption spectra. After background correction, the band center and the full width at half band maximum (FWHM) of each band were determined using the program *PeakFit* by Jandel Scientific.

Autocorrelation analysis

In case of vibrational spectroscopy, the band position, band intensity and bandwidth are known to correlate with the square of the order parameter Q from Landau theory (Salje et al. 2000). Especially in case of dynamic order–disorder transitions, the investigation of bandwidths has proven versatile, whereas changes in band positions and intensities were found to be not that sensitive (Libowitzky and Beran 2004).

To obtain an effective linewidth of the OH-bands of topaz-OH, we used the autocorrelation method (Salje et al. 2000). Therefore, the spectral region 3,650–3,420 cm^{-1} has been selected as the appropriate segment of each primary IR spectrum. A suitable linear baseline between these end points was subtracted from each spectrum. Then, each segment was correlated with itself using the autocorrelation function

$$Corr(\alpha, \omega') = \int \alpha(\omega + \omega')\alpha(\omega)d\omega \quad (1)$$

to produce an autocorrelated spectrum (Salje et al. 2000). The width of the central peak of each autocorrelation spectrum varies with the general width of the bands of the primary IR spectrum. Therefore, it contains the combined information of the linewidth of the overlapping sequence of bands. Within the limit $\omega \rightarrow 0$ the width of the central peak contains the quantitative information of the primary linewidths, which can be extracted by extrapolation. We fitted a Gaussian curve to the central peak around the offset $\omega' = 0$ for successive ranges of ω' between 8 and 30 cm^{-1}. ΔCorr, the FWHM of the Gaussian curve at $\omega' = 0$, is derived by extrapolation using a fourth-order polynomial.

Results

Powder X-ray diffraction

The run products were characterized by powder XRD at room temperature. Topaz-OH was the sole solid phase found. As initial crystal structure for the structure refinement, we took the data reported by Northrup et al. (1994) from the Inorganic Crystal Structure Database (ICSD, FIZ Karlsruhe, http://icsd.FIZ-karlsruhe.de). The refined unit cell parameters were $a = 4.7278(2)$ Å, $b = 8.9302(5)$ Å, $c = 8.4264(4)$ Å and $V = 355.77(3)$ $Å^3$, 2σ–uncertainties given in parentheses. The space group (SG) used for the refinement was *Pbnm*. The obtained values are in good agreement with the data reported by Wunder et al. (1993) and Northrup et al. (1994).

Temperature-dependent IR spectroscopy

IR spectra of the OH-stretching region at 3,740–3,340 cm^{-1} are shown in Fig. 1a for selected temperatures between –196 and 600°C. At room temperature two OH-bands at 3,602 cm^{-1} (ν_1) and 3,525 cm^{-1} (ν_2) are present, together with an unresolved shoulder at the low-energy wing of ν_2 (Wunder et al. 1993, 1999). With increasing temperature, both bands broaden and the band centers approach each other so that at 600°C only one asymmetric broad band at about 3,580 cm^{-1} is visible. The behavior in the low-temperature range, –196 to 30°C, is shown in Fig. 1b. The band's shape gets more distinct at lower temperatures and the shoulder at the low-energy wing of ν_2 becomes increasingly pronounced. The center of ν_1 remains unaffected, whereas ν_2 shifts toward lower wavenumbers. At about –160°C the shape of both bands flattens at the top and two plateaus form, of which each splits with further decreasing temperature into two bands (Fig. 1b). At –196°C one can clearly distinguish between four different bands: ν_{1a}, ν_{1b}, and ν_{2a}, ν_{2b}. Both effects, band splitting at low temperature as well as overlapping of the two bands ν_1 and ν_2 at high temperature, are reversible during heating and cooling along the entire temperature range.

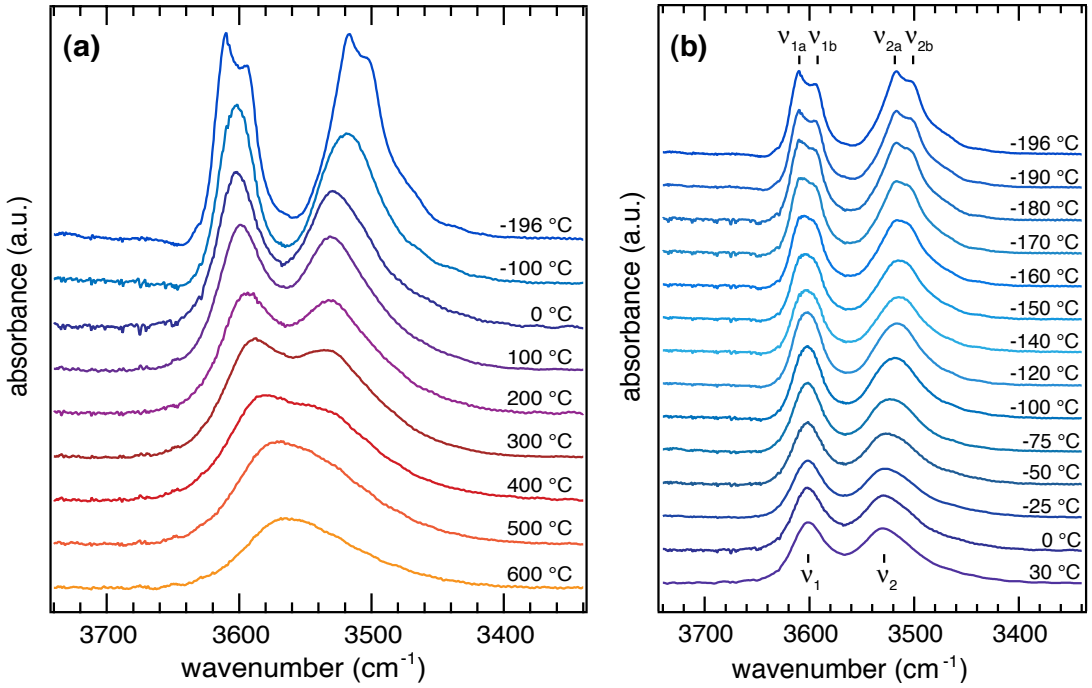

Figure 1: a IR spectra of topaz-OH in the spectral region of the OH-stretching vibrations at selected temperatures between –196 and 600°C. **b** IR spectra of topaz-OH in the same spectral region with focus on low temperature between –196 and 30°C. All spectra are offset for clarity.

Band positions and FWHMs of the low-temperature spectra (Fig. 1b) were determined by peak fitting of the absorption bands in the OH-stretching region. The data were extracted from fits neglecting the band splitting at very low temperatures, i.e., only one band was fitted under each position. This is reasonable because the splitting occurs symmetrically and has no significant effect on the bandwidth. The data are listed in Table 1. The 1σ-uncertainty of the band position and the FWHM is about ± 1.5 cm^{-1}. Figure 2a and b show the behavior of peak position and FWHM of ν_1 and ν_2, respectively, as a function of temperature. The OH-concentration c for each particular OH-band was calculated using the Lambert–Beer-law $c = A/(3 \cdot \epsilon \cdot t)$, where A is the measured absorbance from the particular band in the IR spectrum, ϵ the molar absorption coefficient for water in minerals from Libowitzky and Rossman (1997) and t the film thickness. Taking the spectrum at 30°C as an example, ν_1 represents about 40% and ν_2 about 60% of the total OH-concentration. This implies that the sites are non-equally occupied, which is in agreement with neutron powder diffraction data of topaz-OD at room temperature (Komatsu et al. 2008). In case of the splitted bands at –196°C a further evaluation of the absolute intensities of ν_1 and ν_2, respectively, allowed the following assignment: 55% to ν_{1a} and 45% to ν_{1b}, as well as 64% to ν_{2a} and 36% to ν_{2b}.

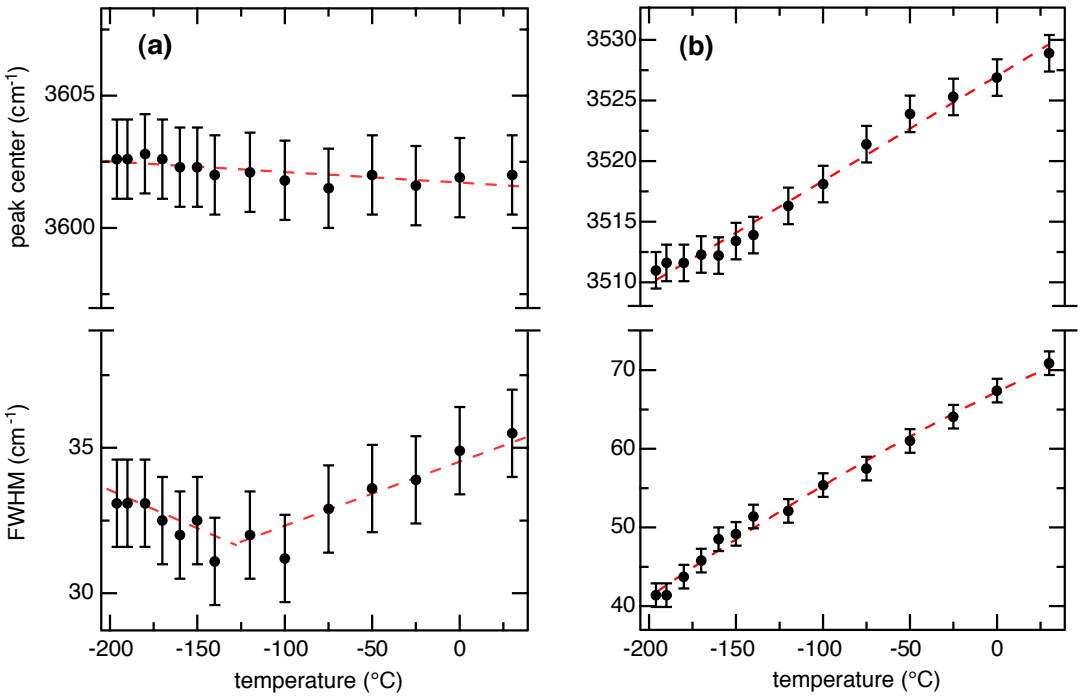

Figure 2: Temperature dependence of the peak position and the FWHM of the OH-stretching bands **(a)** ν_1 and **(b)** ν_2. Data were obtained by fitting only one band at each position (see text for further explanations). Dashed lines are derived from linear fits of the data points and illustrate changes in the slopes.

Autocorrelation analysis

The results from the autocorrelation analysis of the temperature-dependent IR spectra are shown in Fig. 3. The variation of ΔCorr as a function of temperature reveals two steps in the slope, one at about –155°C and another at about 380°C, which can be interpreted as indications of phase transitions. The transition temperature at 380°C is determined by the intersection of two linear fits, but due to the large temperature interval between two adjacent points in Fig. 3, only an approximate value is obtained. The 1σ-uncertainties of ΔCorr are below 1%. The main source of errors in the autocorrelation analysis is the sample preparation. All IR measurements of this study were carried out on the same sample film. A systematic error due to the sample preparation is hence negligible. The uncertainty of ΔCorr comes from the autocorrelation itself.

Table 1. Band positions and FWHMs of the OH-stretching bands ν_1 and ν_2 at low temperatures.

T (°C)	band center ν_1 (cm^{-1})	FWHM ν_1 (cm^{-1})	band center ν_2 (cm^{-1})	FWHM ν_2 (cm^{-1})	r^2
30	3602.0	35.5	3528.9	70.9	0.9957
0	3601.9	34.9	3526.9	67.4	0.9931
–25	3601.6	33.9	3525.3	64.1	0.9942
–50	3602.0	33.6	3523.9	61.0	0.9938
–75	3601.5	32.9	3521.4	57.5	0.9949
–100	3601.8	31.2	3518.1	55.4	0.9926
–120	3602.1	32.0	3516.3	52.1	0.9942
–140	3602.0	31.1	3513.9	51.4	0.9911
–150	3602.3	32.5	3513.4	49.2	0.9910
–160	3602.3	32.0	3512.2	48.5	0.9895
–170	3602.6	32.5	3512.3	45.8	0.9881
–180	3602.8	33.1	3511.6	43.7	0.9876
–190	3602.6	33.1	3511.6	41.4	0.9807
–196	3602.6	33.1	3511.0	41.4	0.9831

1σ-uncertainty of band position and FWHM: 1.5 cm^{-1}
r^2: agreement factors from peak fitting

Discussion

IR spectroscopy

We discuss our experimental results in the light of the predictions derived from ab inito quantum-mechanical calculations (Churakov and Wunder 2004). Applying their notation, we assign the four OH-bands at low temperatures (Fig. 1b) to the following stretching modes, for reasons, which will become clear below: ν_{1a} to O4–H4, ν_{1b} to O4–H1, ν_{2a} to O4–H3 and ν_{2b} to O4–H2. The calculated atomic positions of hydrogen in the crystal structure proposed by Churakov and Wunder (2004) have been reconciled by Komatsu et al. (2008) with those obtained from X-ray and neutron diffraction data of topaz-OH(D) (Northrup et al. 1994; Chen et al. 2005; Komatsu et al. 2008). Accordingly, positions H3 and H4 of Churakov and Wunder's (2004) assignment correspond to H(D)1 and H(D)2 of the terminology of Komatsu et al. (2008).

Below –160 °C, the IR spectra of topaz-OH clearly show four different OH-bands in the spectral region of the OH-stretching vibrations (Fig. 1b), indicating four non-equivalent hydrogen positions. According to Churakov and Wunder's (2004) calculations, the distribution among these four sites is strongly temperature dependent. Their calculations at –218°C predict abandoned H1 and H2 positions, but indicate high proton concentrations in H3 and H4. Both positions, H3 and H4, are half occupied due to H–H repulsion. With increasing thermal energy, the proton mobility increases and more protons enter the H1 and H2 sites, which is in line with our low-temperature IR spectra (Fig. 1b).

From the results of the calculations, we consider H3 and H4 to be the most occupied positions at liquid nitrogen temperature. Our data for the OH-concentrations at this temperature showed higher concentration for ν_{1a} and ν_{2a}. Therefore, we assign ν_{1a} to the O4–H4

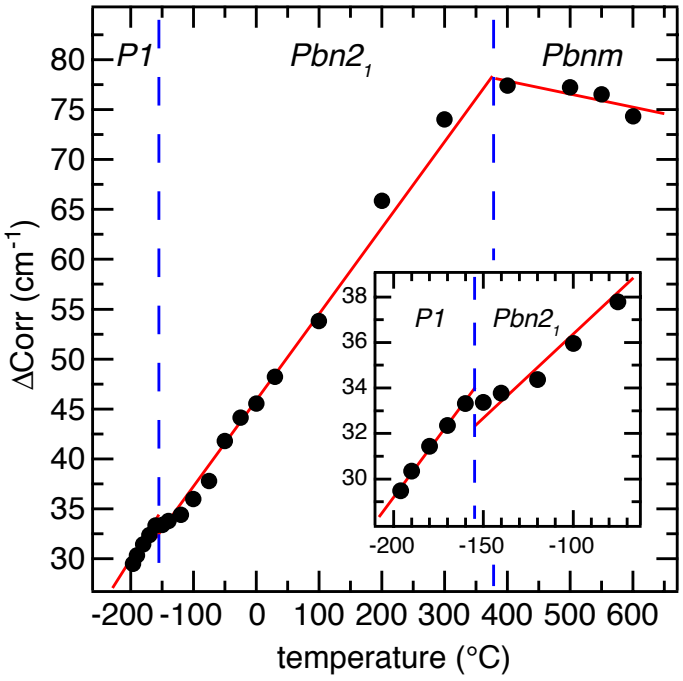

Figure 3: Variation of ΔCorr with temperature obtained from autocorrelation analysis of the IR spectra in the wavenumber range between 3,650 and 3,420 cm^{-1}. Vertical dashed lines indicate approximate transition temperatures of the *P1* ↔ *Pbn2*$_1$ ↔ *Pbnm* order–disorder phase transitions. Errors are within the size of the plotted data points.

and ν_{2a} to the O4–H3 mode. As H1 is closely adjacent to H4 and, accordingly, H2 to H3, ν_{1b} is assigned to O4–H1 and ν_{2b} to O4–H2 mode.

Approaching –160 °C from below results in enhanced occupation of H1 and H2 at the expense of H4 and H3, respectively (Fig. 1b). Accordingly, above –160 °C ν_{1a} and ν_{1b} merge into ν_1, and ν_{2a} and ν_{2b} into ν_2. Following Churakov and Wunder (2004), ν_1 and ν_2 display the superposition of the four bands, because increasing thermal energy allows the protons to switch between the closely adjacent positions. The two positions at room temperature, H(D)1 and H(D)2 after Komatsu et al. (2008), are in turn the superposed positions of H3, H2 and H4, H1, respectively. The small difference between these positions is yet unresolvable by crystal structure analysis. At higher temperatures, the protons switch easily among the four sites, which connote that they are completely disordered. Accordingly, above 400°C the OH-bands ν_1 and ν_2 merge into one superposed band ν_{OH} (Fig. 1a). One can speculate that high-temperature X-ray diffraction possibly detects only one proton position.

Generally, in case of linear or nearly linear hydrogen bonds, the OH-bands shift toward higher wavenumbers with increasing temperature due to extended O–H$\cdots$O distances. Furthermore, the bands broaden with increasing thermal energy as a result of the enhanced oscillation amplitudes of the OH-vibrations. Principally, the OH-band ν_2 follows these common rules (Fig. 2b), though we find that the band's shift and the increase of the FWHM is nonlinear, but of a second-order polynomial. In contrast to that, the temperature-dependent

behavior of the band position and the bandwidth of ν_1 (Fig. 2a) is quite surprising: (1) The position of ν_1 does not change within the error (Fig. 2a), and (2) the FWHM of ν_1 shows a pronounced discontinuity, which is characterized by a minimum of the FWHM at about –140°C (Fig. 2a). One possible explanation of this behavior, another is given in the following section, is a temperature-induced crossover of the two bands underneath ν_1. Crossover means that two bands interchange their positions due to changing conditions (temperature, pressure, $\cdots$) in a way that their paths cross each other. However, such a crossover implies that ν_{1a} is the low-wavenumber band underneath ν_1 at room temperature and that the corresponding O4–H4$\cdots$O4 bond weakens, i.e., with decreasing temperature the O4–H4$\cdots$O4 distance increases, O4–H4$\cdots$O4 strongly bends or O4–H4 forms bonds with further acceptor oxygens.

The effect that decreasing temperature or increasing pressure on crystal structures has is often comparable, because both generally result in volume contraction and therefore shortening of the interatomic distances. Komatsu et al. (2008) investigated the effect of pressure up to 7.5 GPa on the crystal structure of topaz-OD by neutron powder diffraction. With increasing pressure, each of the O–D$\cdots$O distances (following notation after Komatsu et al. 2008) decreased. However, as a result of extremely decreasing O–D–O angles the distances D1$\cdots$O2 and D2$\cdots$O1 increase with increasing pressure. As a consequence, the donor–acceptor interaction strengthens for O4–D1$\cdots$O3, O4–D2$\cdots$O2 and O4–D2$\cdots$O4 and weakens for O4–D1$\cdots$O2 and O4–D2$\cdots$O1 with increasing pressure. From these results, indeed, O4–D2$\cdots$O1, corresponding to O4–H1$\cdots$O1 of Churakov and Wunder (2004), is a possible candidate for the OH-band shift toward higher wavenumbers with decreasing temperature. This hypothesis partly contradicts the results of Churakov and Wunder (2004) in that H1 and not H4 represents ν_{1a} at –196°C. For verification, low-temperature crystal structure analyses on topaz-OD, using neutron diffraction, are strongly needed. However, these measurements go beyond the scope of this study.

Komatsu et al. (2005) determined Raman spectra of topaz-OH in the range of the OH-bands between ambient conditions and 17.3 GPa. With increasing pressure, neither an indication of band splitting nor any unusual discontinuity in the band shift was observed. Hypothetically, in analogy to the low-temperature IR spectra, a band splitting might occur at pressures above 17.3 GPa. Yet, we suggest that the thermally induced hydrogen order–disorder is mainly responsible for the observed band splitting and not the shortening of the interatomic distances due to volume contraction, which is simulated by the applied pressure. This is indicated by simultaneous splitting of ν_1 and ν_2 at the same temperature of about –160°C. A change of O–H$\cdots$O distances with temperature or pressure is known to be strongly anisotropic (Fei 1995) and hence would induce individual band splitting at different temperatures or pressure.

Autocorrelation analysis

Changes in the line width of IR and Raman spectra can conveniently characterize dynamic order–disorder phase transitions. Therefore, reliable FWHM, extracted from spectroscopic data, are required. Low-temperature IR spectra of topaz-OH show four different OH-bands, which overlap with increasing temperature. Manual fitting each single band to determine its line width is difficult and imprecise over the whole temperature range. Fitting two superior

bands, ν_1 and ν_2, works at low temperatures (Table 1, Fig. 2). However, band shifting and broadening as well as merging into one asymmetric broad band above 400°C affect accurate band fitting for the high-temperature spectra. In contrast to conventional peak fitting, the autocorrelation method characterizes bandwidths in phonon spectra with even complex band shape (Salje et al. 2000) and therefore is used here to examine the FWHM changes.

Steps in the slope of ΔCorr reveal possible phase transitions at about –155°C and 380°C (Fig. 3), respectively. A step in the FWHM of ν_1 and ν_2 at low temperature is also observed for the manually fitted data (Fig. 2). Because of the above described difficulties with the band fitting, the determined transition temperature, –140°C, is much less accurate. We suggest changes in symmetry from space group *P1* to $Pbn2_1$ for the low-temperature and from $Pbn2_1$ to *Pbnm* for the high-temperature transition. The low-temperature transition is a static–dynamic transition, whereas the high-temperature transition is caused by disordering of the protons.

Several observations from other studies support our proposed phase transitions, hence the limitations of the methods has to be kept in mind for the interpretation of the results. Diffraction studies are sensitive to long-range order and give crystal structure properties averaged over many unit cells. In contrast, spectroscopic studies focus on short-range order and give informations on the local structure and the crystal chemical properties.

Churakov and Wunder (2004) argued that at low temperature, ordered proton configurations of four non-equivalent H-positions exist and that the protons are almost fixed in their positions due to restricted proton movement. These configurations, essentially observable in the IR spectrum at –196°C, violate all symmetry elements of *Pbnm* and hence have to be assigned to *P1*. Northrup et al. (1994) found two structurally different H-sites by single-crystal XRD on topaz-OH at room temperature. As a result of ordering of the H-atoms, they suggested a symmetry reduction from the centrosymmetic space group *Pbnm* to non-centrosymmtric $Pbn2_1$ due to loss of the mirror plane (001). This assumption was verified by second harmonic generation measurements, which indicated a lack of a center of symmetry (Northrup et al. 1994). Calculations of the proton density distribution at 392°C (Churakov and Wunder 2004) clearly indicate the existence of the mirror plane (001) and thus point to space group *Pbnm* at such high temperature.

Even though there are a number of arguments for two temperature-dependent phase transitions, no indication of symmetry reduction of space group *Pbnm* was ever observed for topaz-OH from crystal structure refinements (Northrup et al. 1994; Chen et al. 2005; Komatsu et al. 2008). This is not surprising, because X-ray or neutron diffraction techniques, especially at room or higher temperatures, give always only informations on long-range order. We, however, assume that the temperature-induced order–disorder phase transitions in topaz-OH only involve the positions of the H-atoms and that the lattice framework itself remains almost static apart from temperature-dependent volume changes. The detection of H-positions is quite challenging, and in case of topaz-OH even more demanding, because the proton positions are closely adjacent and disordered. A temperature-dependent neutron diffraction study on topaz-OD might be able to resolve the four averaged positions and confirm space group *P1* at low temperatures.

Conclusion

The IR spectra at temperatures below –160°C prove the existence of four non-equivalent H-positions in topaz-OH, which were first predicted by Churakov and Wunder (2004) from ab initio quantum mechanical calculations.

Increasing temperature enhances proton movement in the structure and consequently switching between the closely adjacent positions, H4 and H1 as well as H3 and H2. Around room temperature one can only distinguish between two superposed positions corresponding to two broad OH-bands in the IR spectra. Above 400°C the protons are in complete dynamic exchange between the four positions, which is in line with only one asymmetric broad band in the IR spectra.

The temperature-dependent change of the OH-band shapes is caused by a thermally induced hydrogen order–disorder in the structure, whereas the lattice framework remains almost static. The autocorrelation analysis of the IR spectra in the region of the OH-stretching frequencies revealed two order-disorder phase transitions with regard to the H-atoms. At about –155°C the space group changes from *P1* to $Pbn2_1$ and at about 380°C from $Pbn2_1$ to *Pbnm*. The phase transitions are caused by temperature and dynamic average as temperature induces proton movement and an increasingly more symmetric proton density distribution.

Acknowledgments We thank M. Koch-Müller for the help with the film preparation in the DAC and helpful comments, M. Gottschalk for the help with the program for the autocorrelation analysis and W. Heinrich and E. Libowitzky for fruitful discussions. The reviews by Sergey Churakov and an anonymous reviewer helped to improve the manuscript and are highly appreciated. We thank M. Rieder for the effective editorial handling of the manuscript. This work was supported by the German Science Foundation (He 2015/(8-1)) to W. Heinrich within the framework of the Priority Program 1236 "Structures and properties of crystals at extreme pressures and temperatures", which is gratefully acknowledged.

References

Abbott RN Jr (1990) Topaz: energy calculations bearing on the location of hydrogen. Can Mineral 28:827–833

Barton MD (1982) The thermodynamic properties of topaz solid solution and some petrological applications. Am Mineral 67:956–974

Chen J, Lager GA, Kunz M et al (2005) A Rietveld refinement using neutron powder diffraction data of a fully deuterated topaz, $Al_2SiO_4(OD)_2$. Acta Crystallogr E. doi:10.1107/S1600536805034811

Churakov SV, Wunder B (2004) Ab initio calculations of the proton location in topaz-OH, $Al_2SiO_4(OH)_2$. Phys Chem Miner 31:131–141. doi:10.1007/s00269-003-0365-8

Domanik KJ, Holloway JR (1996) The stability and composition of phengitic muscovite and associated phases from 5.5 to 11 GPa: implications for deeply subducted sediments. Geochim Cosmochim Ac 60(21):4133–415. doi:10.1016/S0016-7037(96)00241-4

Fei Y (1995) Thermal expansion. In: Mineral physics and crystallography – a handbook of physical constants. AGU Reference Shelf 2:29–43

Griffiths PR, de Haseth JA (1986) Fourier transform infrared spectroscopy. Wiley, New York

Komatsu K, Kagi H, Okada T et al (2005) Pressure dependence of the OH-stretching mode in F-rich natural topaz and topaz-OH. Am Mineral 90:266–270. doi:10.2138/am.2005.1652

Komatsu K, Kagi H, Marshall WG et al (2008) Pressure dependence of the hydrogen-bond geometry in topaz-OD from neutron powder diffraction. Am Mineral 93:217–227. doi:10.2138/am.2008.2483

Larson AC, von Dreele RB (2004) Generalized structure analysis system. Los Alamos Nat Lab Rep LAUR, 96–748

Libowitzky E, Beran A (2004) IR spectroscopic characterisation of hydrous species in minerals. In: Beran A, Libowitzky E (eds) Spectroscopic methods in mineralogy, EMU notes in mineralogy, vol 6, pp 227–279

Libowitzky E, Rossman GR (1997) IR absorption calibration for water in minerals. Am Mineral 82:1111–1115

Mertz L (1965) Transformation in optics. Wiley, New York

Northrup PA, Leinenweber K, Parise JB (1994) The location of H in the high-pressure synthetic $Al_2SiO_4(OH)_2$ topaz analogue. Am Mineral 79:401–404

Ono S (1998) Stability limits of hydrous minerals in sediment and mid-ocean ridge basalt compositions: implications for water transport in subduction zones. J Geophys Res 103(B8):18253–18267. doi:10.1029/98JB01351

Ono S (1999) High temperature stability limit of phase egg, $AlSiO_3(OH)$. Contrib Mineral Petr 137:83–89. doi:10.1007/s004100050583

Ribbe PH (1982) Topaz. In: Ribbe PH (ed) Orthosilicates. Reviews in Mineralogy, 2rd edn, pp 215–230

Salje E, Carpenter MA, Malcherek, T et al (2000) Autocorrelation analysis of infrared spectra from minerals. Eur J Mineral 12:503–519

Schmidt MW (1995) Lawsonite: upper pressure stability and formation of higher density hydrous phases. Am Mineral 80:1286–1292

Schreyer W (1995) Ultradeep metamorphic rocks: the retrospective viewpoint. J Geophys Res 100(B5):8353–8366. doi:10.1029/94JB02912

Theye T (1988) Aufsteigende Hochdruckmetamorphose in Sedimenten der Phyllit-Quarzit-Einheit Kretas und des Peloponnes. Ph.D. Thesis, University of Braunschweig

Watenphul A, Wunder B, Heinrich W (2009) High-pressure ammonium-bearing silicates: implications for nitrogen and hydrogen storage in the Earth's mantle. Am Mineral 94:283–292. doi: 10.2138/am.2009.2995

Wunder B, Rubie DC, Ross II CD et al (1993) Synthesis, stability, and properties of $Al_2SiO_4(OH)_2$: a fully hydrated analogue of topaz. Am Mineral 78:285–297

Wunder B, Andrut M, Wirth R (1999) High-pressure synthesis and properties of OH-rich topaz. Eur. J. Mineral 11:803–813

Xue X, Kanzaki M, Fukui H et al (2006) Cation order and hydrogen bonding of high-pressure phases in the $Al_3O_3 - SiO_2 - H_2O$ system: an NMR and Raman study. Am Mineral 91:850-861. doi:10.2138/ am.2006.2064

Zhang RY, Liou JG, Shu JF (2002) Hydroxyl-rich topaz in high-pressure and ultrahigh-pressure kyanite quartzites, with retrograde woodhousite, from the Sulu terrane, eastern China. Am Mineral 87:445–453